REMARKS

Claims 2, 5-8, 16-18, 35, 37, and 39-41 will be pending after the entry of the amendment with this response. Claims 1, 11, 12, 19, 22, 25, 26, 33, 34, 36, and 38 have been previously canceled without prejudice in the interest of advancing prosecution. Claim 2 has been amended for clarity. No new matter is introduced by this amendment.

Applicants thank the Examiner for withdrawing certain rejections and objections, and for indicating claims 39-41 are in condition for allowance.

Objections to Claims

The Examiner maintained but has held in abeyance the objections to claims 8 and 16-17 for not being limited to the elected species.

35 USC §112, first paragraph

The examiner maintained rejection of claims 2, 5-8, 16-18, 35, 37, alleging these claims are not enabled by the disclosure of the specification for the full scope of the claims. The Examiner states that the specification does not provide sufficient guidance to enable a skilled artisan to understand and carry out the invention *in vivo*.

The Examiner rejects the pending claims as not enabled, alleging insufficient disclosure for *in vivo* administration. The claims relate generally to methods of promoting dendritic growth. The Examiner states that, because cyclic AMP or gp130 is involved in many cellular activities, and modulating these cellular components would have a far reaching effect. Applicants do not disagree with the reasonableness of the Examiner's statement. However, the claims are to "methods for promoting neuronal cell dendritic growth," not "methods for promoting neuronal cell dendritic growth only, without any other effects." If the compositions recited in the claims promote neuronal cell dendritic growth, and the specification supports those claims, then the claims are enabled.

The Examiner is also concerned that *in vivo* results are not predictable by the *in vitro* data because *in vitro* experiments are carried out with only sympathetic neuronal culture, whereas there are other cell types *in vivo*.

Applicants maintain that the *in vitro* systems used by Applicants reflect *in vivo* utility of a composition. Further, inhibitors of cyclic AMP dependent protein kinase have been seen to have effects on BMP-7 (OP-1) activities in the hands of other investigators as well. Gupta *et al., J. Biol. Chem.* Vol. 274, No. 37, Issue of September 10, pp. 26305–26314, 1999, (Exhibit A) examined the effect of H89, an inhibitor of cyclic AMP dependent protein kinase, on renal branching morphogenesis using explant. The addition of H89 had stimulatory effects in a manner similar to that seen with low doses of BMP-7. Although the tissue is different, the experiment indicates that in a tissue setting, administering cAMP inhibitor has an effect similar to stimulating a morphogen. Accordingly, enhancing morphogen activity to elicit neuronal dendritic growth is reasonably expected to be similar to increasing morphogen activity by administering a morphogen itself.

The Examiner also rejects the claims alleging non-enablement by extending the scope of the claim to methods of treatment of neurodegenerative diseases. Applicants respectfully request that the Examiner consider whether the claims as written, i.e., methods for promoting neuronal cell dendritic growth, are enabled by the specification, and not as methods for treating neurodegenerative diseases, which is not what is being claimed. While many of the neurons at the advanced stage of neurodegenerative diseases are dead or damaged beyond repair, at the initial stage of the disease and in the periphery of the lesion at any stage of the disease, there are neurons that are damaged but may survive by the methods claimed in the instant application. As such, Applicants respectfully disagree with the Examiner's allusion that whether the claimed methods are enabled based on the unpredictability of treatment of neurodegenerative diseases.

The Examiner alleged claims 2, 5, 8, 35 and 37 were not enabled because the experiments show that, in the absence of a morphogen inhibitor in the form of exogenous neuropoietic cytokines such as CNTF or LIF, recited inhibitors have no effect. Applicants amended claim 2 (and accordingly all claims dependent on claim 2) to more clearly recite this condition. The specification

described the addition of morphogen inhibitors into the culture system, supporting the recitation of an exogenous morphogen inhibitor. It is known that CNTF, for example, is expressed by glial cells within the central and peripheral nervous systems and is released when injury occurs nearby. (see Exhibit B, Abstract, Sleeman et al., Pharm Acta Helv. 2000 Mar;74(2-3):265-72) Therefore Applicants submit that when the methods are carried out in vivo, there inherently is found CNTF. The present amendment simply articulates what is already there.

Applicants submit that the amended claims are supported by the specification, and respectfully request that the rejection on this ground be withdrawn.

In view of the above amendment, Applicant believe the pending application is in condition for allowance.

Applicant believes no additional fee is due with this response. However, if an additional fee is due, please charge our Deposit Account No. 18-1945, under Order No. JJJ-P01-569 from which the undersigned is authorized to draw.

Dated: October 25, 2007

Respectfully submitted,

By _____

Erika Takeuchi
Registration No.: 55,661
ROPES & GRAY LLP
1211 Avenue of the Americas
New York, New York 10036
(212) 596-9000
(212) 596-9090 (Fax)
Attorneys/Agents For Applicant

EXHIBIT A

THE JOURNAL OF BIOLOGICAL CHEMISTRY
Vol. 274, No. 37, Issue of September 10, pp. 26305–26314, 1999
Printed in U.S.A.

Protein Kinase A Is a Negative Regulator of Renal Branching Morphogenesis and Modulates Inhibitory and Stimulatory Bone Morphogenetic Proteins*

(Received for publication, February 8, 1999, and in revised form, June 1, 1999)

Indra R. Gupta‡§, Tino D. Piscione‡§, Silviu Grisaru‡§, Tien Phan‡§, Marina Macias-Silva§, Xiaopeng Zhou¶, Catharine Whiteside¶, Jeffrey L. Wrana§, and Norman D. Rosenblum‡§‖

From the ‡Division of Nephrology, The Hospital for Sick Children, University of Toronto, Toronto, Ontario, the §Program in Developmental Biology, The Hospital for Sick Children, University of Toronto, Toronto, Ontario M5G 1X8, and the ¶Division of Nephrology, The Toronto Hospital, University of Toronto, Toronto, Ontario M5G 1X8, Canada

Protein kinase A (PKA) regulates morphogenetic responses to bone morphogenetic proteins (BMPs) during embryogenesis. However, the mechanisms by which PKA regulates BMP function are unknown. During kidney development, BMP-2 and high doses of BMP-7 inhibit branching morphogenesis, whereas low doses of BMP-7 are stimulatory (Piscione, T. D., Yager, T. D., Gupta, I. R., Grinfeld, B., Pei, Y., Attisano, L., Wrana, J. L., and Rosenblum, N. D. (1997) *Am. J. Physiol.* 273, F961–F975). We examined the interactions between PKA and these BMPs in embryonic kidney explants and in the mouse inner medullary collecting duct-3 model of collecting duct morphogenesis. H-89, an inhibitor of PKA, stimulated branching morphogenesis and enhanced the stimulatory effect of low doses of BMP-7 on tubule formation. Furthermore, H-89 rescued the inhibition of tubulogenesis by BMP-2 (or high doses of BMP-7) by attenuating BMP-2-induced collecting duct apoptosis. In contrast, 8-bromo-cAMP, an activator of PKA, inhibited tubule formation and attenuated the stimulatory effects of low doses of BMP-7. To determine mechanisms underlying the interdependence of BMP signaling and PKA activity, we examined the effect of PKA on the known signaling events in the BMP-2-dependent Smad1 signaling pathway and the effect of BMP-2 on PKA activity. PKA did not induce endogenous Smad1 phosphorylation, Smad1-Smad4 complex formation, or Smad1 nuclear translocation. In contrast, BMP-2 increased endogenous PKA activity and induced phosphorylation of the PKA effector, cAMP-response element-binding protein, in a PKA-dependent manner. We conclude that BMP-2 induces activation of PKA and that PKA regulates the effects of BMPs on collecting duct morphogenesis without activating the known signaling events in the BMP-2-dependent Smad1 signaling pathway.

Branching morphogenesis, defined as growth and branching of epithelial tubules during embryonic development, arises in the kidney through reciprocal mesenchymal-epithelial tissue interactions between the mesenchymal metanephric blastema and the epithelial ureteric bud (and its derivative collecting ducts) (1). These interactions are mediated by secreted peptide growth factors. Members of the bone morphogenetic protein (BMP)[1] family, a subset of the TGF-β superfamily, are expressed in a temporal and spatial pattern consistent with their role as regulators of tubular growth and branching (2, 3). BMP-2 inhibits renal branching morphogenesis, whereas BMP-7 is stimulatory at low doses and inhibitory at higher doses (3). Although a growing body of evidence suggests that signals derived from inhibitory and stimulatory BMPs, as well as other growth factors, are integrated by the ureteric bud/collecting duct cells to determine the number and phenotype of tubules (4), the intracellular events that act in concert with these signals are largely undefined.

Protein kinase A (PKA), an intracellular kinase, has been implicated in the control of morphogenesis in diverse nonrenal tissues including the central nervous system (5, 6), the eye (7), and the limb (8, 9). Within these tissues, PKA interacts with growth factor signaling pathways to regulate morphogenetic responses to BMPs (7–9). Within the embryonic limb, BMP-2-mediated stimulation of chondrogenesis is dependent on PKA (9). Furthermore, the mechanism underlying the interdependence between PKA and BMP-2 signaling within the limb may be controlled by BMP-2 because treatment with BMP-2 induces PKA activity (9).

The function of PKA during kidney morphogenesis is undefined. However, evidence in cell culture models suggests a role for PKA in growth factor signaling in the kidney. In the Madin-Darby canine kidney cell model of tubulogenesis, PKA modulates responses to hepatocyte growth factor (HGF), a known regulator of renal branching morphogenesis (10). Additionally, in renal mesangial cells, TGF-β stimulates PKA by a cAMP independent mechanism (11), which provides further evidence that PKA can act downstream of TGF-β superfamily members.

We demonstrate here that PKA inhibits renal branching morphogenesis and modulates the effects of both inhibitory and

* This work was supported by grants from The Hospital for Sick Children Research Training Center (to I. R. G. and S. G.), the Hospital for Sick Children Clinician-Scientist Training Program, the Molly Towell Perinatal Research Foundation and the Kidney Foundation of Canada Fellowship Program (to T. D. P.), the Medical Research Council of Canada (to C. W.), the Medical Research Council of Canada Fellowship Program (to M. M.-S.), the National Cancer Institute of Canada, Terry Fox Fund and Medical Research Council of Canada (to J. L. W.), and the Medical Research Council of Canada and Kidney Foundation of Canada (to N. D. R.). The costs of publication of this article were defrayed in part by the payment of page charges. This article must therefore be hereby marked "*advertisement*" in accordance with 18 U.S.C. Section 1734 solely to indicate this fact.

‖ To whom correspondence should be addressed: Division of Nephrology, The Hospital for Sick Children, 555 University Ave., Toronto, Ontario M5G 1X8, Canada. Tel.: 416-813-5667; Fax: 416-813-6271; E-mail: norman.rosenblum@sickkids.on.ca.

[1] The abbreviations used are: BMP, bone morphogenetic protein; PKA, protein kinase A; HGF, hepatocyte growth factor; 8-Br-cAMP, 8-bromo-cAMP; DIC, differential interference contrast; TUNEL, terminal deoxynucleotidyl transferase-mediated labeling; FBS, fetal bovine serum; DMEM-F12, Dulbecco's modified Eagle's medium-Ham's F-12 nutrient mixture; CREB, cAMP-response element-binding protein; TGF, transforming growth factor; PBS, phosphate-buffered saline; mIMCD, mouse inner medullary collecting duct; PKI, protein kinase A inhibitor; DAB, diaminobenzidine tetrahydrochloride.

stimulatory BMPs. Using embryonic renal explants and an *in vitro* cell culture model of tubulogenesis, we demonstrate that inhibition of PKA rescues ureteric buds or collecting ducts from the inhibitory effects of BMPs by decreasing tubular cell apoptosis. Consistent with these effects, activation of PKA abrogates the stimulatory effects of low dose BMP-7. To determine whether the effect of PKA is mediated by known signaling events in the BMP-dependent Smad1 signaling pathway, we showed that PKA has no effect on endogenous Smad1 phosphorylation, Smad1-Smad4 complex formation, or Smad1 nuclear translocation. To determine whether the dependence of inhibitory BMPs on PKA is mediated by regulation of the PKA signaling pathway by BMPs, we demonstrated that BMP-2 increases endogenous PKA activity and induces phosphorylation of its downstream effector, cAMP-response element-binding protein (CREB). Taken together, our results show that PKA acts via a pathway parallel to ligand-induced Smad1 to inhibit renal branching morphogenesis and that PKA activity is positively regulated by BMP-2.

MATERIALS AND METHODS

Embryonic Kidney Organ Culture and Treatment with Recombinant Proteins—Murine embryos were surgically resected from embryonic (E) day 12 pregnant CD1 mice and the kidneys were cultured as described previously (3). Explants were grown in Dulbecco's modified Eagle's medium-Ham's F-12 nutrient mixture (DMEM-F12) with Richter's modification (Life Technologies, Inc.) containing 50 μg/ml transferrin (Sigma) and either no ligand, 5 nM BMP-2 (kindly provided by Genetics Institute), 0.25 nM BMP-7 (originally named OP-1) (kindly provided by Creative Biomolecules), 30 nM BMP-7 alone, or combinations of each of these growth factors with 5–10 μM H-89 (Calbiochem) for 48–60 h. Explants were fixed in 4% fomaldehyde for 10 min, washed four times with PBS, and then embedded in paraffin. 5-μm tissue sections were stained with hematoxylin and eosin and imaged by light microscopy.

Mouse Inner Medullary Collecting Duct (mIMCD-3) Model of Tubulogenesis—Tubulogenesis assays were performed in type I collagen in 96-well culture plates using mIMCD-3 cells, as described previously (3). Cell culture medium was supplemented with either 5 nM BMP-2, 0.25 nM BMP-7, 30 nM BMP-7, 25 ng/ml HGF (Collaborative Biomolecules), or combinations of these growth factors with either 1–50 μM H-89, 0.0001–500 μM 8-bromo-cAMP (8-Br-cAMP), or 1–100 nM protein kinase A inhibitor (PKI) amide 14–22 (Calbiochem). After 48 h, gels were fixed in 4% formaldehyde, washed in PBS, and then imaged by differential interference contrast (DIC) microscopy. The number of tubular structures in an area of standardized dimensions was determined in four randomly selected positions of the gel for each treatment condition by an observer blinded to the treatment condition, as described previously (3). Data were analyzed using the Statview statistical analysis program (version 4.01; Abacus Concepts, Berkeley, CA). The mean differences between the various treatment groups was analyzed in a Student's *t* test (two-tailed).

Immunofluorescence—To study nuclear translocation of Smad1, mIMCD-3 cells were grown in monolayer on glass coverslips in DMEM-F12 culture medium supplemented with 0.2% fetal bovine serum (FBS), penicillin (100 units/ml), streptomycin (100 units/ml) in 5% CO_2 at 37 °C for 12 h. Cells were treated for 1 h with either 5 nM BMP-2, 5 μM H-89, or 5 μM 8-Br-cAMP or combinations of BMP-2/H-89 or BMP-2/8-Br-cAMP and then fixed in 4% formaldehyde. After three washes in PBS, the cells were permeabilized with methanol for 15 min at room temperature and then blocked with 10% goat serum and 3% bovine serum albumin in PBS for 1 h at room temperature. Cells were incubated with anti-Smad 1 antibody (12) (1:50 dilution) overnight at 4 °C, washed with PBS, and then incubated with fluorescein isothiocyanate-conjugated goat anti-rabbit antibody (Jackson Immunologicals; 1:200 dilution) for 60 min at room temperature. Coverslips were mounted and imaged using a Zeiss Axioskop confocal laser microscope.

Immunoidentification of mIMCD-3 Cellular Proteins—mIMCD-3 cells were labeled with [^{32}P]phosphate as described previously (13). Briefly, phosphate-labeled cells were incubated in DMEM-F12 with 0.2% FBS in the presence of either 5 nM BMP-2, 5 μM H-89, 5 μM 8-Br-cAMP, BMP-2/H-89, or BMP-2/8-Br-cAMP. Cell lysates were subjected to immunoprecipitation with anti-Smad1 antibody followed by adsorption to protein A-Sepharose (Amersham Pharmacia Biotech). Immunoprecipitated proteins were washed, separated by SDS-polyacrylamide gel electrophoresis, and visualized by autoradiography.

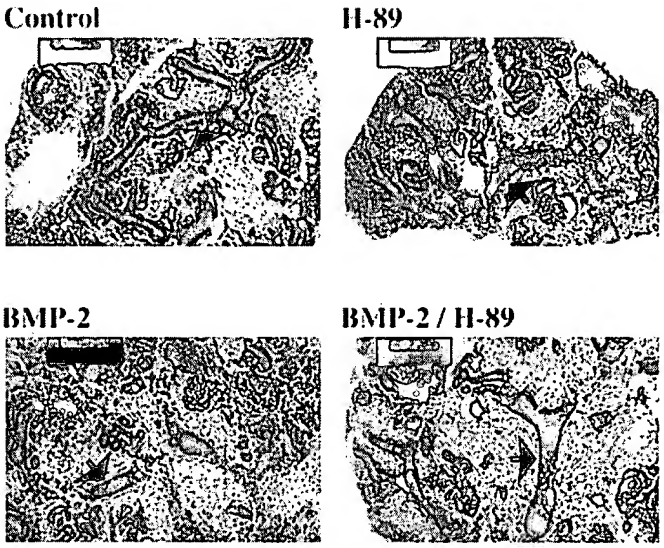

FIG. 1. **Effect of PKA on branching morphogenesis in embryonic kidney explants.** E12 embryonic mouse kidneys were cultured in serum-free medium containing H-89, BMP-2, or both. After 48 h, paraffin-embedded 5-μm tissue sections were generated from fixed explant tissue. Images are of hematoxylin-eosin-stained tissue sections. Sections were imaged at × 100 magnification. *Bar*, 75 μm. *Arrows* mark the position of ureteric bud/collecting duct structures.

To analyze Smad1-Smad4 complex formation, mIMCD-3 cells were incubated in DMEM-F12 with 0.2% FBS in the presence of either 5 nM BMP-2, 5 μM H-89, 5 μM 8-Br-cAMP, BMP-2/H-89, or BMP-2/8-Br-cAMP. Cell lysates were subjected to immunoprecipitation with either anti-Smad1 antibody or anti-Smad4 antibody followed by adsorption to protein A-Sepharose. Immunoprecipitated proteins were washed, separated by SDS-polyacrylamide gel electrophoresis, and transferred to nitrocellulose membranes. Analysis by immunoblotting was performed using a rabbit anti-Smad4 antibody (12) (1:1000 dilution) followed by anti-rabbit horseradish peroxidase (1:10,000) and chemiluminescence.

To analyze phosphorylation of CREB, cell lysates were immunoblotted using a rabbit anti-phospho-CREB (Ser-133) antibody (New England Biolabs) (1:1000 dilution) followed by anti-rabbit horseradish peroxidase (1:2,000) and chemiluminescence. Identical blots were probed with a rabbit anti-CREB antibody (New England Biolabs) (1:1000 dilution) to measure CREB protein expression.

In Vitro Kinase Assay for PKA Activity—mIMCD-3 cells were grown in DMEM-F12 with 0.2% FBS and treated with 5 nM BMP-2, 5 μM 8-Br-cAMP, 5 μM H-89, 8-Br-cAMP/H-89, or BMP-2/H-89. Cell lysates were prepared by suspending the cells in cold extraction buffer (25 mM Tris-HCl, pH 7.4, 0.5 mM EDTA, 0.5 mM EGTA, 10 mM β-mercaptoethanol, 1 μg/ml leupeptin, 1 μg/ml aprotinin) and then homogenized using a Dounce homogenizer. Cell lysates were centrifuged, and then the supernatant was used in a nonradioactive assay for cAMP-dependent protein kinase (PKA assay system, Promega). The amount of protein added to the kinase assay was standardized by measuring absorption by cell lysates at 280 nm using a Hewlett-Packard UV spectrophotometer. Phosphorylated and unphosphorylated forms of the PKA peptide substrate were separated by agarose gel electrophoresis and imaged by UV light.

TUNEL Assay—*In situ* TUNEL assays were performed in embryonic kidney explants and collagen gels using commercially available reagents (Apop Tag kit, Oncor). E12 embryonic kidneys were cultured for 2 days in Richter's modified DMEM-F12 in the presence of 10 μM H-89, 5 nM BMP-2, or both. Deparaffinized tissue sections were treated with proteinase K followed by 3% hydrogen peroxide to quench endogenous peroxidase activity. Sections were preincubated with 100 μl of terminal deoxynucleotidyl transferase equilibration buffer for 15 min at 37 °C and then incubated with 100 μl of terminal deoxynucleotidyl transferase mixed in reaction buffer according to the manufacturer's instructions. The reaction was stopped by immersing slides in 300 mM NaCl, 30 mM sodium citrate buffer, pH 8.0 (stop/wash buffer), for 30 min at 37 °C. Sections were blocked in blocking buffer for 1 h and subsequently treated with 100 μl of sheep monoclonal anti-digoxigenin F(ab) fragments antibody (Roche Molecular Biochemicals) diluted 1:20 in blocking buffer for 1 h at room temperature. After washing sections in PBS, 100 μl of DAB substrate diluted 1:10 in 1× DAB buffer was added for

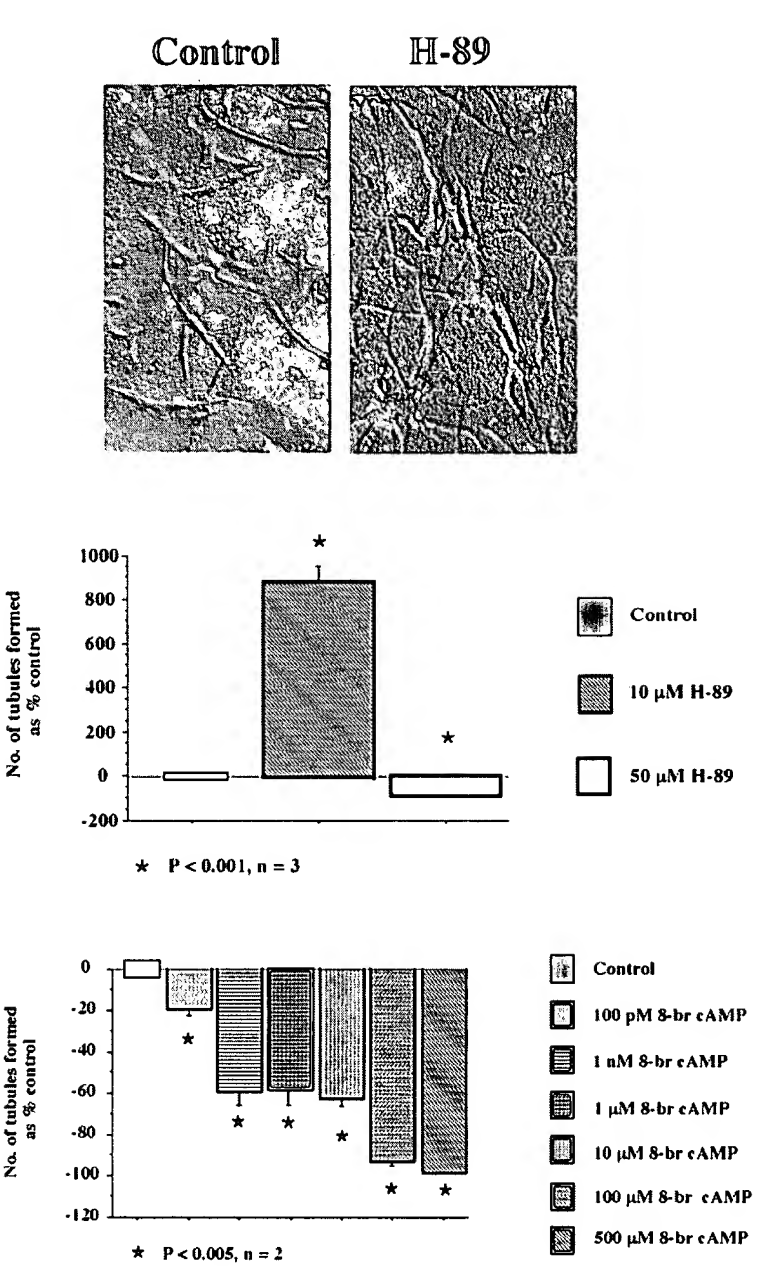

FIG. 2. **Effect of PKA on mIMCD-3 tubulogenesis.** mIMCD-3 cells were cultured in type I collagen for 48 h in the presence of serum alone or increasing doses of 8-Br-cAMP or H-89. *A*, DIC images of tubules formed under control conditions and after treatment with 10 μM H-89 (magnification, × 100). *B* and *C*, dose-response analysis of the number of tubules formed in the presence of increasing doses of H-89 or 8-Br-cAMP. Number of tubules is expressed as a percentage of control (serum alone). 10 μM H-89 stimulated tubule formation (883% stimulation, $p < 0.001$), whereas 50 μM H-89 was inhibitory secondary to induction of cell death (88% inhibition, $p < 0.001$). 8-Br-cAMP was inhibitory at all concentrations tested.

5–7 min and then sections were rinsed in distilled water. Sections were then counterstained with hematoxylin and *Dolichos biflorus* agglutinin and mounted with DPX mountant (VWR Scientific).

Collagen gels containing mIMCD-3 cells were individually transferred from wells of a 96-well culture plate to 1.5-ml microcentrifuge tubes and treated with 0.2% trypsin at 37 °C for 2 h. Gels were washed four times in PBS, preincubated in terminal deoxynucleotidyl transferase equilibration buffer for 1 h, and subsequently treated with terminal deoxynucleotidyl transferase in reaction buffer for 5 h at 37 °C. The reaction was terminated in stop/wash buffer for 30 min at 37 °C. Cells were left overnight in blocking buffer at 4 °C and then incubated with 100 μl of anti-digoxigenin antibody diluted 1:20 in blocking buffer for 4 h at 37 °C. After four 5-min washes in PBS, cells were stained with 3-amino-9-ethylcarbazole (Zymed Laboratories Inc.) for 10–20 min and rinsed with PBS. Cells were counterstained with 1 μg/ml bisbenzamide (Hoechst No. 33258; Sigma) for 30 min at 4 °C, followed by two washes in PBS. Cells were directly imaged by DIC and fluorescent microscopy.

RESULTS

PKA Controls Renal Branching Morphogenesis and Modulates the Effects of BMPs in Embryonic Kidney Explants—We investigated the role of PKA and its interaction with BMPs that control renal morphogenesis because PKA has been implicated in the control of cellular responses to BMPs (9). To determine whether PKA regulates renal development, we manipulated its activity in embryonic kidney explants and identified alterations in collecting duct morphogenesis. H-89 is a direct reversible antagonist of the activated catalytic subunit of PKA (14, 15). E12 murine metanephric explants were grown for 48 h in the presence or absence of 10 μM H-89. As shown in Fig. 1, in control explants, elongated, branched ureteric bud/collecting ducts were formed. H-89 induced stimulation of branching morphogenesis with the formation of wider, longer, and more branched tubules. To determine the function of PKA in the context of the inhibitory BMPs, BMP-2, and high dose BMP-7, kidney explants were grown for 48 h in the presence of 5 nM BMP-2, 30 nM BMP-7, H-89/BMP-2, or H-89/BMP-7. Treatment of explants for 48 h with 5 nM BMP-2 inhibited collecting duct formation resulting in short, unbranched tubules that failed to grow into the peripheral cortex. However, H-89 reversed the BMP-2 effect and promoted the formation of longer and more branched collecting tubules. Similar results were obtained in the cultures treated with high doses of BMP-7 and H-89/

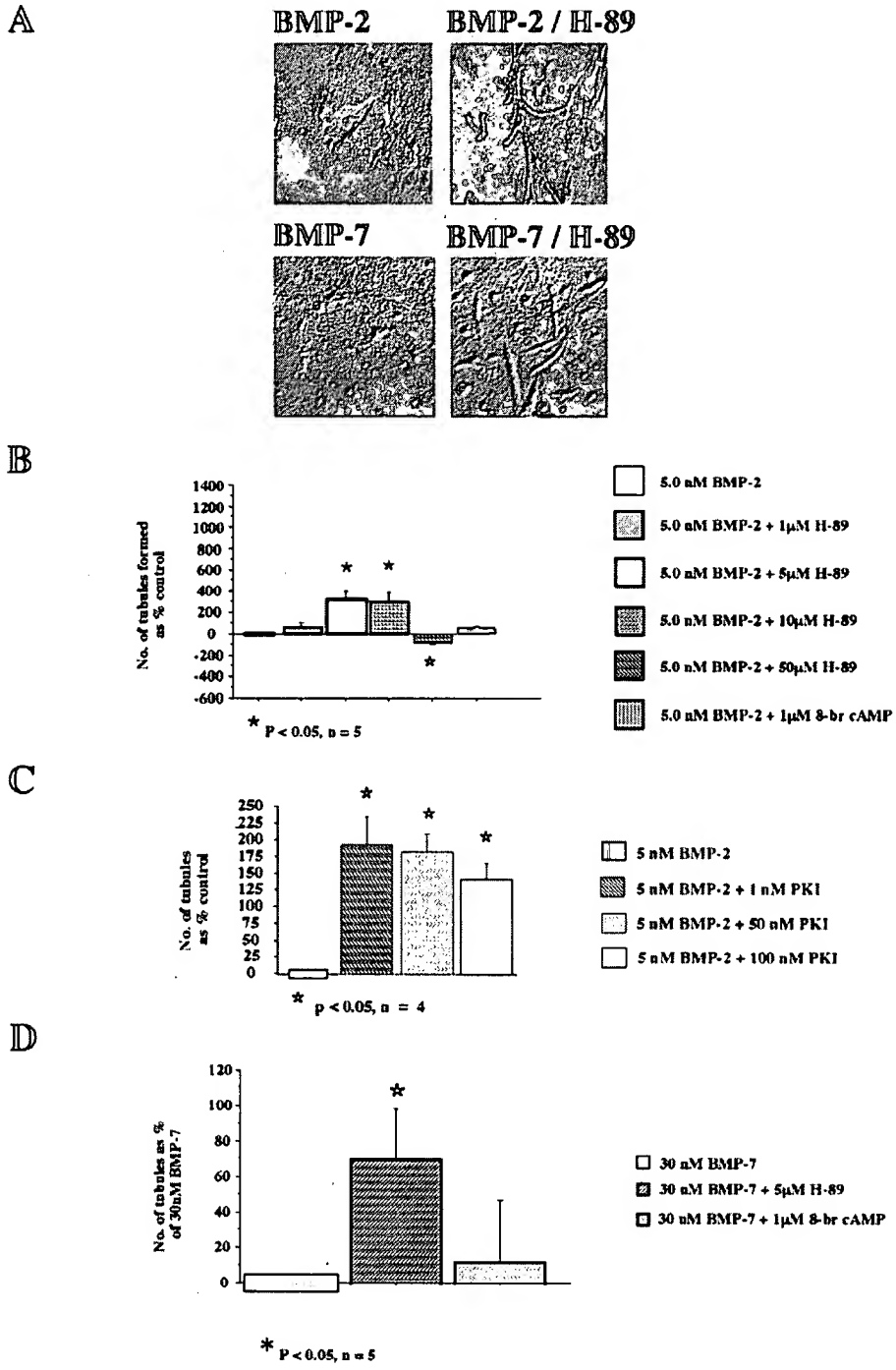

FIG. 3. **Effect of PKA on BMP-mediated inhibition of branching morphogenesis.** mIMCD-3 cells were cultured in type I collagen for 48 h in the presence BMP-2, BMP-7, or H-89 in combination with either BMP-2 or BMP-7. *A*, DIC images of tubules (magnification, × 100). Treatment with 5 nM BMP-2 generated a small number of short, unbranched tubules. Addition of 10 μM H-89 to BMP-2-treated cultures generated numerous long, slender, highly branched tubules. Treatment with 30 nM BMP-7 completely inhibited tubule formation. Addition of 10 μM H-89 to BMP-7 rescued BMP-7-mediated inhibition, generating tubules with few branches. *B–D*, dose-response analysis of the number of tubules formed in the presence of increasing dose of H-89 or PKI with a constant concentration of BMP-2 or BMP-7. *B*, number of tubules is expressed as a percentage of control (5 nM BMP-2). H-89 rescued the number of tubules formed in the presence of BMP-2 in a dose-dependent manner. In contrast, 1 μM 8-Br-cAMP had no stimulatory effect. *C*, number of tubules is expressed as a percentage of control (5 nM BMP-2). PKI rescued the number of tubules formed in the presence of BMP-2. *D*, number of tubules is expressed as a percentage of control (30 nM BMP-7). 5 μM H-89 rescued the number of tubules formed in the presence of 30 nM BMP-7 (70% stimulation, $p < 0.05$). In contrast, 1 μM 8-Br-cAMP exerted no significant stimulatory effect.

BMP-7. We were not able to demonstrate enhancement of tubule formation by H-89 in the presence of low doses of BMP-7 because BMP-7, alone, exerted a potent stimulatory effect (3) (data not shown). In summary, these results suggest that antagonism of PKA promotes branching morphogenesis in embryonic explants and attenuates the inhibitory effects of BMPs.

Direct Effects of PKA during Collecting Duct Morphogenesis in Vitro—The cellular complexity of the organ culture explant precludes analysis of PKA effects on specific cells within the collecting duct system. We have used mIMCD-3 cells, which are derived from the terminal inner medullary collecting duct of the SV40 transgenic mouse and form branched tubules in three dimensional matrices (3, 16), to investigate the direct effects of PKA on branching morphogenesis. mIMCD-3 cells were seeded in type I collagen, cultured for 48 h in the presence of H-89 or the specific activator of PKA, 8-Br-cAMP (17), and then imaged by DIC microscopy. Tubules treated with H-89 were longer and more highly branched than tubules grown under control conditions consistent with our observations in renal explants (Fig. 2*A*). Tubules treated with 8-Br-cAMP were similar in phenotype to control tubules (data not shown). Because we also observed an effect of H-89 and 8-Br-cAMP on tubule number, we quantitated the number of tubules formed in the presence of these agents. 10 μM H-89 increased tubule number by 883% compared with control ($p < 0.001$) (Fig. 2*B*). At 50 μM H-89, no tubules were formed secondary to toxic effects on the cell, as indicated by morphologic evidence of cell death. In contrast, 8-Br-cAMP exerted a dose-dependent inhibitory effect with 61% inhibition at 1 nM ($p < 0.005$) (Fig. 2*C*). Taken together, the opposing effects of H-89 and 8-Br-cAMP on mIMCD-3 tubulogenesis suggest that PKA directly controls renal branching morphogenesis at the level of tubule number.

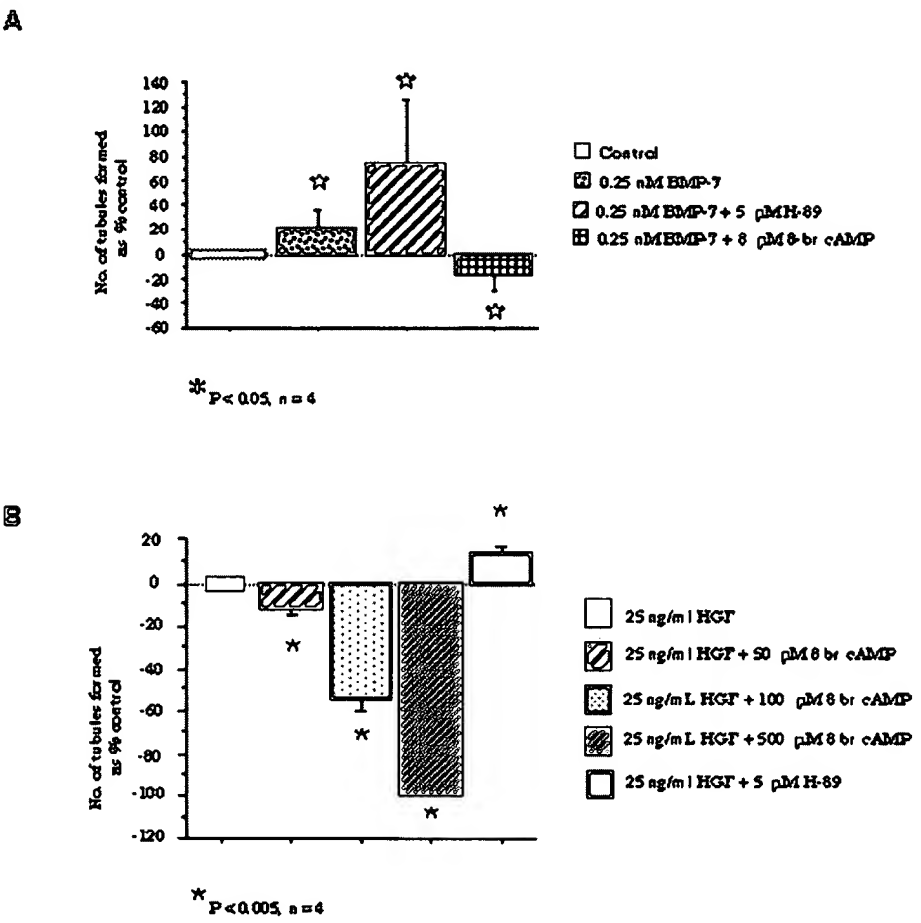

FIG. 4. **Effect of PKA on the stimulation of branching morphogenesis by BMP-7 and HGF.** mIMCD-3 cells were cultured in type I collagen for 48 h in the presence of stimulatory doses of BMP-7 or HGF, alone and in combination with either H-89 or 8-Br-cAMP. *A*, effect of PKA on stimulation by BMP-7. Number of tubules is expressed as a percentage of control (serum alone). 0.25 nM BMP-7 increased tubule formation by 21%. Addition of H-89 in the presence of 0.25 nM BMP-7 enhanced tubule formation by 73% compared with control and by 52% compared with BMP-7 alone. In contrast, addition of 8 μM 8-Br-cAMP inhibited tubule formation by 16% compared with control and by 37% compared with BMP-7 alone ($p < 0.05$). *B*, effect of PKA on stimulation by HGF. Number of tubules is expressed as a percentage of control (25 ng/ml HGF). 8-Br-cAMP inhibited HGF-stimulated tubulogenesis at all concentrations tested. In contrast, H-89 enhanced HGF-stimulated tubule formation.

PKA Modulates the Effects of BMPs in Vitro on Renal Branching Morphogenesis—Having determined that PKA potently modulates renal branching morphogenesis, we determined its interactions with the BMP signaling pathway. The results of our experiments in embryonic kidney explants (Fig. 1) suggested that BMP-mediated inhibition of ureteric bud/collecting duct growth and branching is dependent on PKA activity because antagonism of PKA rescued the inhibitory effects of BMPs. To test this more directly, we determined the interactions between BMPs and PKA in the mIMCD-3 culture model. Addition of H-89 to cultures treated with 5 nM BMP-2 induced a rescue of BMP-2-mediated inhibition (Fig. 3*A*). Quantitation of these effects showed that 5 μM H-89 enhanced tubule formation in the presence of BMP-2 by 328% ($p < 0.05$) (Fig. 3*B*). To obtain independent evidence that H-89 was acting to inhibit PKA, we determined the effects of the PKI amide 14–22 in our *in vitro* model of tubulogenesis. PKI rescued tubule formation in BMP-2-treated cultures in a dose-dependent manner (maximum effect: 1 nM, 190%, $p < 0.05$) (Fig. 3*C*). In contrast to H-89 and PKI, when 5 nM BMP-2 was combined with 1 μM 8-Br-cAMP, tubulogenesis was inhibited to the same degree as observed with BMP-2 treatment alone (Fig. 2*B*). Because BMP-2 exerts a strong inhibitory effect on tubule formation, we were not able to determine whether 8-Br-cAMP acted synergistically with BMP-2 to inhibit. Similarly, addition of H-89 to mIMCD-3 cultures treated with high doses (30 nM) of BMP-7 induced a rescue of BMP-7-mediated inhibition by 70% ($p < 0.05$) (Fig. 3*D*). However, when 30 nM BMP-7 was combined with 1 μM 8-Br-cAMP, the inhibitory effect of BMP-7 was unchanged. In summary, these data indicate that inhibitory BMPs, including BMP-2 and high dose BMP-7, are dependent on PKA to exert their inhibitory effects on renal branching morphogenesis.

BMP-7, at low doses (<0.25 nM), acts to stimulate renal branching morphogenesis (3). To determine whether PKA might also play a role in modulating this stimulatory pathway, we tested the interactions between H-89, 8-Br-cAMP and low doses of BMP-7. H-89 enhanced BMP-7 stimulated tubulogenesis by 52% compared with BMP-7 alone ($p < 0.05$) (Fig. 4*A*). In contrast, 8-Br-cAMP decreased the stimulatory effect of BMP-7 by 37% ($p < 0.05$). These results indicate that PKA negatively modulates stimulation by BMP-7 and are consistent with the dependence of inhibitory BMPs on PKA. To determine whether PKA modulates other stimulatory pathways, including those downstream of receptor tyrosine kinases, we tested the interaction of H-89 or 8-Br-cAMP with HGF. As shown in Fig. 4*B*, H-89 enhanced the stimulatory effect of HGF on tubulogenesis by 13% ($p < 0.005$). In contrast, 8-Br-cAMP exerted a dose-dependent inhibitory effect in the presence of HGF. Taken together, these data suggest that PKA modulates stimulatory pathways mediated by both receptor tyrosine (HGF) and receptor serine/threonine (BMPs) kinases.

Inhibition of PKA Activity Blocks BMP-2-mediated Collecting Duct Apoptosis—Our studies in embryonic kidney explants and in the mIMCD-3 model of branching morphogenesis indicate that PKA acts at a morphogenetic level to alter the phenotype of renal collecting tubules. The morphogenetic pathway for any particular tissue or structure is derived from a composite of cellular events, such as cell proliferation, apoptosis, cell shape change and cell migration (18). Because antagonism of PKA rescues BMP-mediated inhibition of tubulogenesis, we determined whether this was due to a change in collecting duct cell number. Specifically, we determined the effects of BMP-2, H-89, and both together on apoptosis in the developing collect-

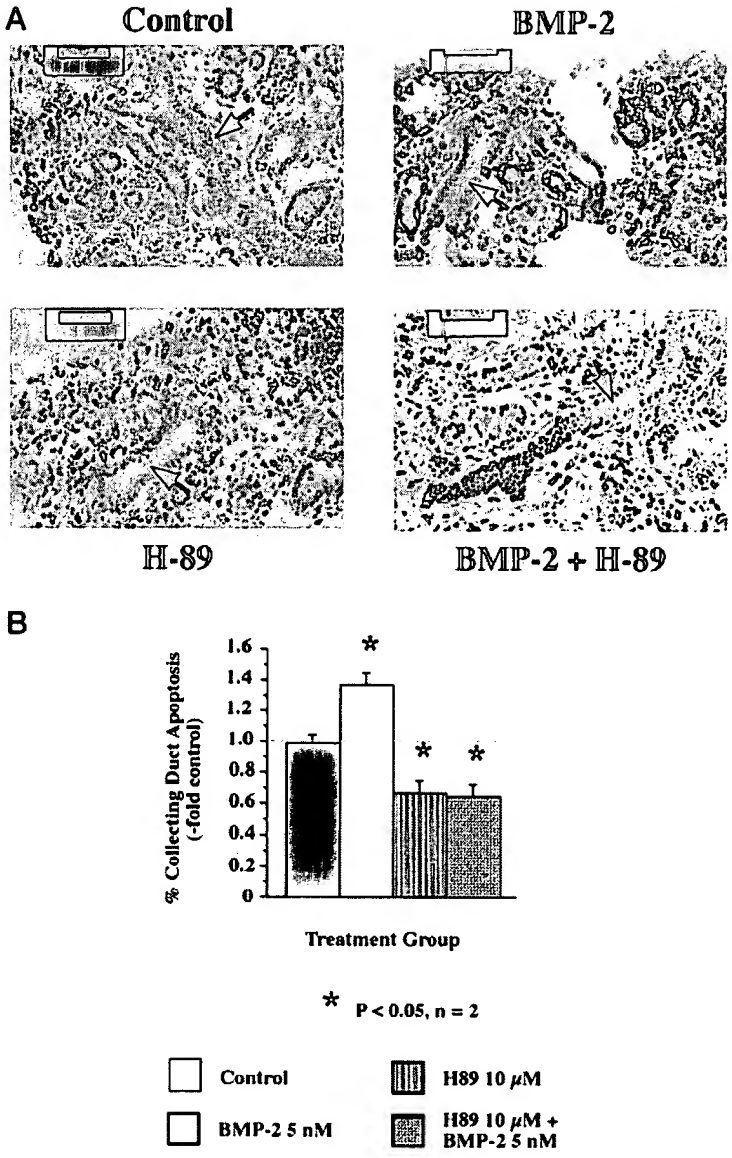

FIG. 5. **Effect of PKA on BMP-2-mediated ureteric bud/collecting duct cell apoptosis.** *A* and *B*, E12 embryonic mouse kidneys were cultured in serum-free medium containing 5 nM BMP-2 or both 5 nM BMP-2 and 10 μM H-89. After 48 h, paraffin-embedded 5 μm tissue sections were generated from fixed explant tissue. Apoptotic cells were identified in ureteric buds/collecting ducts, identified by staining with *Dolichos biflorus* agglutinin, using an *in situ* TUNEL assay. *A*, bright field images of TUNEL-stained tissue sections counterstained with hematoxylin. The *arrows* mark the position of ureteric buds/collecting ducts. Sections were imaged at × 400 magnification. A limited number of brown TUNEL-positive cells are present in the collecting system of control explants. Treatment with BMP-2 markedly attenuated development of collecting tubules and increased the number of apoptotic cells in these tubules. Treatment with H-89 induced the formation of large, elongated, and highly branched collecting tubules in which apoptotic cells were rarely observed. Treatment with H-89 in the presence of BMP-2 partially rescued the BMP-2 phenotype and decreased the number of apoptotic cells. *B*, quantitation of apoptosis. The ratio of apoptotic cells to the total number of ureteric bud/collecting duct cells in each tissue section was determined. Data are presented as fold change from control (no BMP-2 or H-89). *C* and *D*, mIMCD-3 cells were cultured in type I collagen for 48 h in the presence of serum alone, BMP-2, H-89, or both BMP-2 and H-89. *C, upper panels,* immunofluorescence images of cultures stained with bisbenzamide to identify individual cells. *Lower panels,* DIC images of black colored cells stained with 3-amino-9-ethylcarbazole during a TUNEL assay. *D*, quantitation of apoptosis. The ratio of apoptotic cells to the total number of mIMCD-3 cells in each image was determined. Data are presented as fold change from control (no BMP-2 or H-89).

ing system. E12 embryonic kidney explants were cultured for 48 h in the presence of 5 nM BMP-2, 10 μM H-89, or both. Histologic sections were then prepared from fixed tissue, and ureteric bud/collecting ducts were identified by staining with *Dolichos biflorus* agglutinin, and apoptotic cells were assessed using an *in situ* TUNEL assay (Fig. 5*A*). BMP-2 markedly enhanced the number of apoptotic cells in collecting tubules and decreased tubule formation. In contrast, H-89 induced the formation of large, elongated, and highly branched collecting tubules in which apoptotic cells were rarely observed. Treatment with H-89 in the presence of BMP-2 partially rescued the BMP-2 phenotype and ameliorated the extent of apoptosis. The effect of these treatments on ureteric bud/collecting duct apoptosis was quantitated by determining the ratio of apoptotic cells to the total number of ureteric bud/collecting duct cells in each tissue section. Because there was no statistically significant difference between the number of ureteric bud or collecting duct cells in control compared with BMP-2-treated explants (control, 774 ± 60 *versus* BMP-2, 604 ± 110; $p = 0.21$), and in BMP-2 compared with BMP-2/H89-treated explants (BMP-2, 604 ± 110 *versus* BMP-2/H-89, 503 ± 212; $p = 0.53$), the ratio of apoptotic to the total number of cells reflects only the effect of these treatments on apoptosis. As shown in Fig. 5*B*, BMP-2 increased apoptosis by 1.4-fold compared with control (no ligand), whereas antagonism of PKA attenuated collecting duct apoptosis in embryonic kidney explants by 0.4-fold compared with control and by 2.0-fold compared with BMP-2-treated explants ($p < 0.05$). Treatment with H-89 in the presence of BMP-2 attenuated apoptosis to an extent similar to that observed with H-89 alone (2.0-fold) ($p < 0.05$).

To determine the direct effects of H-89 on BMP-2-treated collecting duct cells, we measured mIMCD-3 cell apoptosis in three-dimensional cultures. mIMCD-3 cells were cultured for 48 h in the presence of BMP-2, H-89, or both. Apoptotic cells were identified by the TUNEL assay (Fig. 5*C*). Because the numbers of cells at the time cultures were initiated and after 48 h of culture did not differ, the ratio of the number of TUNEL positive cells to the total number of cells (that is, the number of bisbenzamide-staining cells) reflects only an effect on apoptosis. As shown in Fig. 5*D*, treatment with BMP-2 induced a 3-fold increase in apoptosis compared with control (BMP-2, 11.0 ± 2.1% *versus* control, 3.7 ± 0.7%, $p = 0.002$). This BMP-2 induced increase was similar in degree to that observed after culture of mIMCD-3 cells in serum-free medium (12.3 ± 1.8%). In contrast, treatment with H-89 had no significant effect on apoptosis and totally abrogated the pro-apoptotic effect of BMP-2. Taken together, our results in embryonic kidney explants and in the mIMCD-3 model of collecting duct morpho-

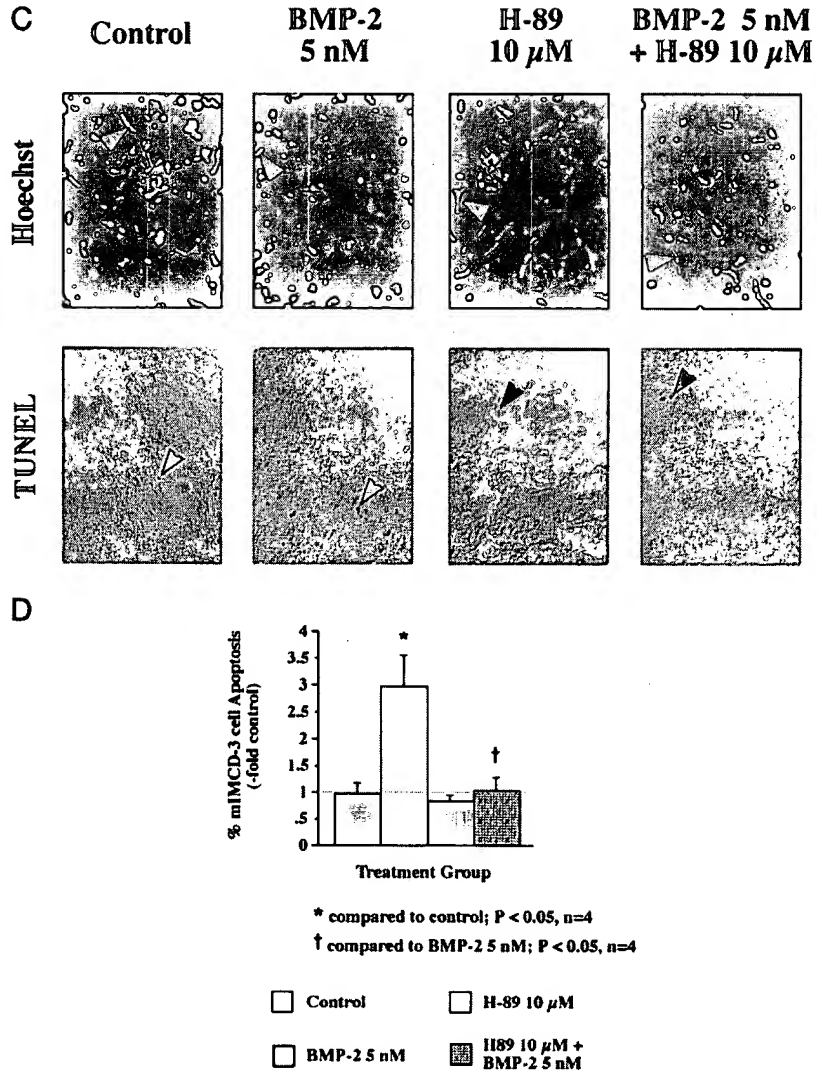

FIG. 5—*continued*

genesis demonstrate that inhibition of PKA, alone and in the presence of BMP-2, protects the collecting duct cell from undergoing apoptosis.

Interaction of PKA with Intracellular Signaling Events Downstream of BMP-2—We have demonstrated that PKA modulates morphogenetic and cellular responses to BMPs. Our results provide a basis for determining the interactions between PKA and BMPs at a molecular level. Several events downstream of BMP/cell surface receptor molecular complexes have been described (19). Specifically, activated BMP receptor phosphorylates the cytoplasmic protein Smad1. Phosphorylated Smad1 complexes to Smad4 and then Smad1 translocates to the nucleus, where it is postulated to act as a transcription factor. Because BMP-mediated inhibition of branching morphogenesis is dependent on PKA, we hypothesized that PKA could induce one or more events downstream of the BMP receptor. Likewise, we predicted that inactivation of PKA would be disruptive to BMP signaling.

First, we investigated the effects of PKA on BMP-2-induced Smad1 phosphorylation in mIMCD-3 cells. mIMCD-3 cells were labeled with [^{32}P]phosphate and then treated with either 5 nM BMP-2, 5 μM 8-Br-cAMP, 5 μM H-89, BMP-2/H-89, or BMP-2/8-Br-cAMP for 1 h. Cellular proteins were immunoprecipitated with anti-Smad1 antibody, and the immunoprecipitated proteins were then analyzed by SDS-polyacrylamide gel electrophoresis. As shown in Fig. 6*A*, BMP-2 induced a marked increase in Smad1 phosphorylation as indicated by both an increase in radioactive signal and a decrease in the electrophoretic migration of Smad1. This mobility shift is a direct result of phosphorylation of residues in the MH2 domain, inducing a conformational change in the protein and causing it to migrate more slowly than unphosphorylated Smad1 (19). In contrast, under basal conditions, phosphorylation of Smad1 occurs at residues located outside of the MH_2 domain, does not result in a conformational change, and does not result in formation of Smad1-Smad4 complexes and nuclear translocation (12). Treatment with 8-Br-cAMP or H-89 did not induce a shift in Smad1 mobility. Moreover, treatment either with 8-Br-cAMP or with H-89 in addition to BMP-2 did not modify the increase in Smad1 phosphorylation or the shift in Smad1 mobility seen in cultures treated with BMP-2 alone. The small degree of variation in the intensity of the Smad1 protein bands observed reflects fluctuations in the yield of Smad1 isolated in the immunoprecipitation procedure. Taken together, these data indicate that the BMP-2 and PKA pathways do not converge at the level of Smad1 phosphorylation.

Second, we determined the effect of PKA on BMP-2 induced Smad1-Smad4 complex formation in mIMCD-3 cells (Fig. 6*B*). For this, we subjected lysates from mIMCD-3 cells to anti-Smad1 immunoprecipitation followed by immunoblotting with an anti-Smad 4 antibody as described previously (12). Under basal conditions, whereas cell lysates contained Smad4 protein (Fig. 6*B, Basal*), Smad 4 was not detected in association with Smad1, indicating that Smad1-Smad4 complexes do not exist

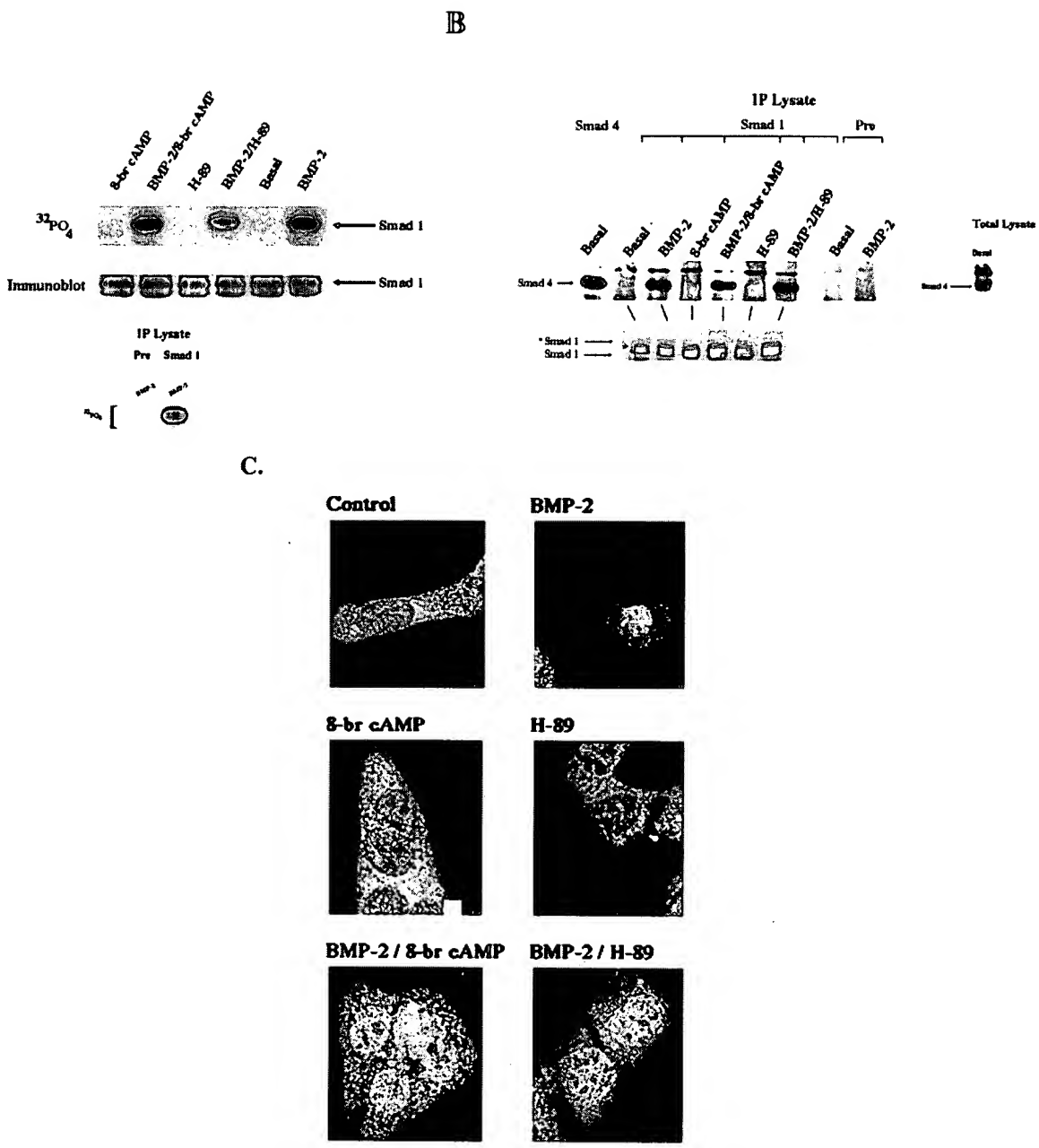

FIG. 6. **Effect of PKA on signaling events induced by BMP-2.** mIMCD-3 cells were incubated in 5% FBS + DMEM-F12 and then treated for 1 h with either 5 nM BMP-2, 5 μM 8-Br-cAMP, 5 μM H-89, BMP-2/H-89, or BMP-2/8-Br-cAMP. *A*, effect of PKA on BMP-2-dependent Smad1 phosphorylation. *Upper panel,* mIMCD-3 cells were labeled with [^{32}P]phosphate during treatment with BMP-2/H-89/8-Br-cAMP. After immunoprecipitation with an antibody to Smad1, proteins were analyzed by SDS-polyacrylamide gel electrophoresis and autoradiography. BMP-2 induced phosphorylation of Smad1 (*arrow*) as indicated by increased [^{32}P]phosphate labeling and decreased mobility compared with basal conditions (no ligand). *Middle panel,* total Smad1 expression in each treatment condition. Smad1 was identified in cell lysates by immunoblotting. *Lower panel,* specificity of anti-Smad1 antibody. mIMCD-3 cells were treated with BMP-2, and cellular proteins were labeled with [^{32}P]phosphate. Proteins were immunoprecipitated with either preimmune rabbit serum or Smad 1 antibody. *B*, effect of PKA Smad 1-Smad 4 complex formation. *Upper panel,* protein lysates were immunoprecipitated with an antibody to Smad4 (total lysate and basal), an antibody to Smad1 (basal, BMP-2, 8-Br-cAMP, BMP-2/8-Br-cAMP, H-89, and BMP-2/H-89), or preimmune sera (basal and BMP-2) and then analyzed by immunoblotting using antibody to Smad4 (*arrow*). *Lower panel,* immunoblot analysis with anti-Smad1 antibody of cellular proteins immunoprecipitated with anti-Smad1 antibody. A band corresponding to the nonphosphorylated form of Smad 1 is seen in all lanes. A slower migrating protein, marked by an *asterisk,* is seen in the BMP-2, BMP-2/8-Br-cAMP, and BMP-2/H-89 treatment groups. This band corresponds to the phosphorylated form of Smad1. *C*, effect of PKA on BMP-2-dependent Smad 1 nuclear translocation in mIMCD-3 cells. Immunostaining was performed using an antibody to Smad1, followed by a fluorescein-conjugated secondary antibody. Images were obtained by confocal laser microscopy (× 480 magnification).

under basal conditions. Similar to these controls, cells treated with 8-Br-cAMP or H-89 did not contain Smad1-Smad4 complexes. In contrast, treatment with 5 nM BMP-2 for 60 min resulted in the formation of Smad1-Smad4 complexes, and the efficiency of association was unaffected by 8-Br-cAMP or H-89. Taken together, these data indicate that the BMP-2 and PKA pathways do not converge at the level of Smad1-Smad4 complex formation.

Smad1-Smad4 complexes translocate to the nucleus, where they function to activate BMP-responsive genes. Thus, we determined whether PKA altered BMP-2 induced Smad1 cytoplasmic to nuclear translocation in collecting duct cells using immunofluorescence and confocal laser microscopy (60 cells analyzed/treatment group) (Fig. 6*C*). Under basal conditions, Smad1 protein was detected in a punctate distribution throughout the cytoplasm of mIMCD-3 cells similar to previous

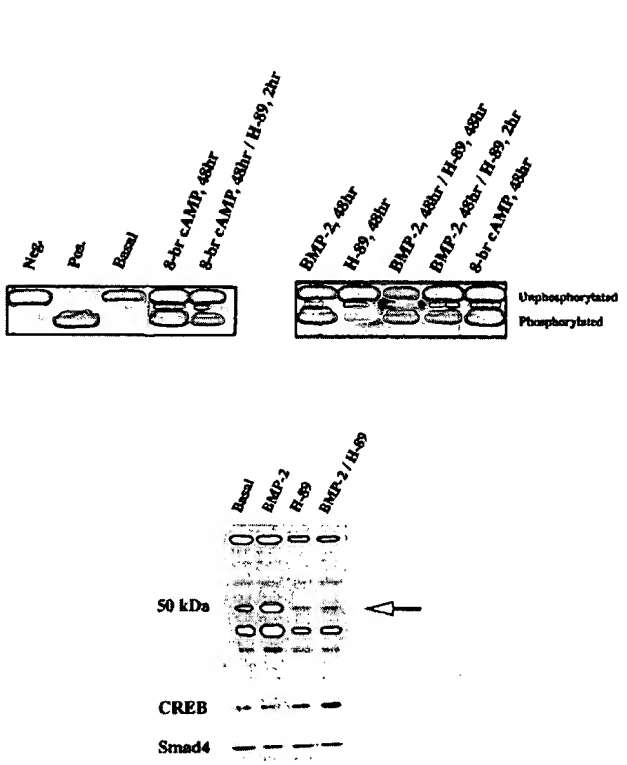

FIG. 7. **PKA and CREB activity in mIMCD-3 cells and effect of BMP-2.** *A*, protein cell lysates were prepared from mIMCD-3 cells and tested for the ability to phosphorylate a PKA-specific peptide in a nonradioactive assay. The phosphorylation state of the peptide was examined by agarose gel electrophoresis. Phosphorylated peptide is positively charged, whereas unphosphorylated peptide is negatively charged. Under basal conditions, PKA activity is low. Treatment with 5 μM 8-Br-cAMP for 48 h activated PKA. In contrast, treatment with 5 μM H-89 attenuated the stimulatory effect of 8-Br-cAMP. Treatment with BMP-2 for 48 h induced PKA activation. *B*, protein cell lysates were tested for the presence of phospho-CREB by immunoblotting proteins isolated from cell lysates with a rabbit anti-phospho-CREB (Ser-133) antibody. Increase in CREB phosphorylation (*arrow*) by BMP-2 is inhibited by co-incubation H-89.

reports for transiently expressed Smad5 (20) and Smad2/3 (21, 22). However, after a 60-min treatment with 5 nM BMP-2, translocation of Smad1 protein was identified by a shift in fluorescent signal from cytoplasm to nucleus in 78% cells analyzed. No signal was detected using preimmune antisera and fluorescein-conjugated secondary antibody (data not shown). Treatment with either 5 μM 8-Br-cAMP or with 5 μM H-89 alone did not induce Smad1 nuclear translocation and did not interfere with BMP-2 induced Smad1 nuclear translocation. Taken together, our experiments indicate that activation of PKA alone does not induce any of the known steps in the BMP-2 pathway. Furthermore, although antagonism of PKA is dominant over the inhibitory effect of BMP-2 on renal branching morphogenesis, it does not disrupt the known biochemical events that are activated in response to BMP-2. These findings suggest that PKA controls the actions of BMP-2 via a parallel signal transduction pathway.

BMP-2 Induces Activation of PKA and the PKA Effector, CREB, in Collecting Duct Cells—Because the inhibitory effect of BMP-2 on renal branching morphogenesis requires PKA activation, and PKA cannot induce BMP-2-mediated signaling events, we hypothesized that BMP-2 positively regulates PKA, thereby regulating its own activity. We investigated this possibility by measuring PKA kinase activity in collecting duct cells. Under basal conditions, PKA activity, as measured by the phosphorylated state of a PKA-specific target peptide, was low (Fig. 7*A*). However, after 10 min of treatment of mIMCD-3 cells with BMP-2, we observed a modest increase in the phosphorylated fraction of the PKA substrate peptide, suggesting increased PKA kinase activity (data not shown). Because we observed the effects of BMP-2 on collecting duct morphogenesis 48 h after cell cultures were established (Figs. 1 and 3*A*), we determined the effect of BMP-2 on PKA activity at this time point. At 48 h, BMP-2 markedly increased PKA activity, which was inhibited by either a short (2 h) or long (48 h) co-incubation with H-89. Induction of PKA activity by BMP-2 was qualitatively similar to that observed after treatment for 48 h with 5 μM 8-Br-cAMP alone (Fig. 7*A*). To determine whether BMP-2 also positively regulates molecules known to function as transcription factors downstream of PKA, we measured phosphorylation of CREB, a PKA substrate (23). Treatment with BMP-2 induced phosphorylation of CREB within 1 h of treatment (Fig. 7*B*). This induction was completely abrogated by treatment with H-89, indicating that PKA is required for BMP-2-mediated phosphorylation of CREB. Taken together, these results demonstrate that PKA and CREB are positively regulated by BMP-2.

DISCUSSION

Several types of evidence strongly suggest that members of the BMP family regulate renal branching morphogenesis. The spatial and temporal expression pattern of BMP-2 and BMP-7 is consistent with their role in modulating the inductive tissue interactions that control branching morphogenesis (2). Mutational inactivation of Bmp-7 causes kidney maldevelopment, including abnormal branching morphogenesis (24, 25). Recombinant BMP-2 and BMP-7 protein control branching morphogenesis in embryonic kidney explants and in the mIMCD-3 model of collecting duct morphogenesis. Interestingly, these BMPs exert specific and dose-dependent effects. BMP-2 is inhibitory, whereas BMP-7 stimulates at low doses (<0.5 nM) and inhibits at higher doses (3). The stimulatory effects of BMP-7 taken together with the phenotype of the Bmp-7 −/− mouse suggest that low dose BMP-7 acts via a stimulatory signaling pathway. In contrast, high doses of BMP-7 and BMP-2 act via the inhibitory Smad 1 signaling pathway.[2] The ureteric bud or collecting duct cells exist within a complex environment of growth factors, including BMPs, and must integrate these diverse signals to form a tubular network. PKA is an intracellular kinase that interacts with both receptor tyrosine kinase (10) and serine/threonine kinase pathways in several tissue types, including the central nervous system (5, 6), the eye (7), and the limb (8). In this work, we show that PKA directly controls renal branching morphogenesis and, within this context, modifies the morphogenetic effects of stimulatory and inhibitory BMPs, and HGF. Our results in an *in vitro* culture model of tubulogenesis and in embryonic renal explants demonstrate that PKA directly controls renal branching morphogenesis. When PKA is activated, tubulogenesis is inhibited, whereas when PKA is antagonized, tubulogenesis is markedly enhanced. Our work also shows that PKA modifies specific growth factor-induced signaling events in the collecting duct cell. PKA inhibits the stimulatory effect of low dose BMP-7 and HGF. Consistent with these effects, antagonism of PKA in the presence of either stimulatory factor further enhances tubulogenesis. In addition, antagonism of PKA rescues the inhibitory effects of BMP-2 and high dose BMP-7. These observations suggest that PKA functions to modulate the cellular response to stimulatory and inhibitory signals during renal branching morphogenesis.

We have demonstrated the effect of PKA on collecting duct formation at a morphogenetic level. Tubule formation requires a unique combination of cellular events including cell prolifer-

[2] I. R. Gupta, M. Macias-Silva, S. Kim, X. Zhou, C. Whiteside, J. L. Wrana, N. D. Rosenblum, submitted for publication.

ation, apoptosis, cell shape change, and cell movement. Our morphogenetic data suggest that PKA exerts an effect on tubular cell number, as indicated by increased tubule formation. Indeed, our results in embryonic kidney explants demonstrate that antagonism of PKA significantly decreases collecting duct apoptosis and abrogates the apoptotic effect of BMP-2. Thus, the protubulogenic effect of H-89 and PKI may arise secondary to an increase in the population of collecting duct cells as a direct result of decreased cellular apoptosis. Further studies will be required to identify other cellular events that may be implicated in the control of tubulogenesis by PKA.

We have examined the function of PKA at a molecular level within the BMP pathway. Our morphogenetic data suggest that BMP-2 and high dose BMP-7 are dependent on PKA. Events downstream of BMP cell surface receptors have been well characterized (19). The cytoplasmic protein Smad1 plays a central role in these events. Smad1 is phosphorylated as a result of BMP/receptor complex formation. This, in turn, permits its translocation to the nucleus. We determined that activation of PKA does not induce Smad1 signaling. Likewise, antagonism of PKA in the presence of BMP-2-induced signaling did not disrupt Smad1 activity. These results suggest that PKA interacts, directly or indirectly, with BMP signaling at the level of the cell nucleus. Such an interaction could be mediated either by PKA itself or one of its downstream targets. The best characterized downstream nuclear target of PKA is CREB (reviewed in Ref. 26). Activation of the PKA catalytic subunit leads to phosphorylation of CREB at serine 133, which allows recruitment of the coactivator CREB-binding protein and binding of this complex to cAMP-response element DNA sequences (23). The possibility that PKA controls BMP-mediated gene transcription is supported by the observation that the BMP-2 homologue dpp stimulates transcription of the ultrabithorax gene in *Drosophila* by inducing CREB binding to a cAMP-response element-responsive element (27). Indeed, the ability of TGF-β-inducible Smads (Smad2, Smad3, and Smad4) to interact with CREB-binding protein has recently been demonstrated (28–31). These observations suggest that the Smad and PKA signaling pathways converge to coordinate gene expression during renal branching morphogenesis. Further studies are required to identify genes that are targeted by CREB-binding protein-BMP-inducible Smad complexes.

Our results that indicate that PKA kinase activity is low in mIMCD-3 cells under basal conditions and that BMP-2 positively regulates PKA and CREB provides insight into the mechanisms that underlie tubulogenesis during renal development. These findings suggest that PKA activity is low in ureteric bud or collecting duct cells that are not exposed to BMP-2 (or inhibitory doses of BMP-7), thus promoting tubulogenesis. However, in areas of tissue where collecting ducts are exposed to inhibitory BMPs, the activity of the PKA signaling pathway is increased, thus promoting inhibition of tubulogenesis.

The mechanism by which BMP-2 activates PKA remains to be determined. PKA activation was originally described as being dependent on cAMP induction (reviewed in Ref. 26). However, recent evidence demonstrates that cAMP-independent activation of PKA can occur via the association of the catalytic subunit of PKA with IkB-a or IkB-b in a NF-kB-IkB-PKAc complex (32). Signals that cause the degradation of IkB release the catalytic subunit of PKA, thereby activating it. Interestingly, TGF-β has recently been reported to induce PKA kinase activity by a cAMP-independent mechanism that is not yet fully characterized (11). Future studies aimed at determining the interactions between BMP signaling intermediates, PKA, and other intracellular proteins will provide insight into the mechanisms that underlie the induction of PKA by BMP-2 in collecting duct cells.

The spatial and temporal patterning of the renal collecting system is precisely controlled (1). Our previous work, as well as that of others, suggests that this development is controlled simultaneously by stimulatory and inhibitory peptide growth factors. Our current work provides insight into how these signals are integrated within the collecting duct cell and provide a basis for further investigating the genetic control of tubulogenesis.

Acknowledgments—BMP-2 was provided via a material transfer agreement with Genetics Institute. BMP-7 (OP-1) was provided via a material transfer agreement with Creative Biomolecules.

REFERENCES

1. Saxen, L. (1987) *Organogenesis of the Kidney*, pp. 51–87, Cambridge University Press, Cambridge, United Kingdom
2. Dudley, A. T., and Robertson, E. J. (1997) *Dev. Dyn.* **208,** 349–362
3. Piscione, T. D., Yager, T. D., Gupta, I. R., Grinfeld, B., Pei, Y., Attisano, L., Wrana, J. L., and Rosenblum, N. D. (1997) *Am. J. Physiol.* **273,** F961–F975
4. Lechner, M. S., and Dressler, G. R. (1997) *Mech. Dev.* **62,** 105–120
5. Hammerschmidt, M., Bitgood, M. J., and McMahon, A. P. (1996) *Genes Dev.* **10,** 647–658
6. Epstein, D. J., Marti, E., Scott, M. P., and McMahon, A. P. (1996) *Development* **122,** 2885–2894
7. Pan, D., and Rubin, G. M. (1995) *Cell* **80,** 543–552
8. Lepage, T., Cohen, S. M., Diaz-Benjumea, F. J., and Parkhurst, S. M. (1995) *Nature* **373,** 711–715
9. Lee, Y.-S., and Chuong, C.-M. (1997) *J. Cell. Physiol.* **170,** 153–165
10. Santos, O. F. P., Moura, L. A., Rosen, E. M., and Nigam, S. K. (1993) *Dev. Biol.* **159,** 535–548
11. Wang, L., Zhu, Y., and Sharma, K. (1998) *J Biol. Chem.* **273,** 8522–8527
12. Macías-Silva, M., Hoodless, P. A., Tang, S. J., Buchwald, M., and Wrana, J. L. (1998) *J. Biol. Chem.* **273,** 25628–25636
13. Wrana, J. L., Attisano, L., Wieser, R., Ventura, F., and Massague, J. (1994) *Nature* **370,** 341–347
14. Chijiwa, T., Mishima, A., Hagiwara, M., Sano, M., Hayashi, K., Inoue, T., Naito, K., Toshioka, T., and Hidaka, H. (1990) *J. Biol. Chem.* **265,** 5267–5272
15. Hidaka, H., Inagaki, M., Kawamoto, S., and Sasaki, Y. (1984) *Biochemistry* **23,** 5036–5041
16. Cantley, L. G., Barros, E. J. G., Gandhi, M., Rauchman, M., and Nigam, S. K. (1994) *Am. J. Physiol.* **267,** F271–F280
17. Orellana, S. A., and McKnight, G. S. (1992) *Proc. Natl. Acad. Sci. U. S. A.* **89,** 4726–4730
18. Larsen, E., and McLaughlin, H. M. G. (1987) *BioEssays* **7,** 130–131
19. Hoodless, P. A., Haerry, T., Abdollah, S., Stapleton, M., O'Connor, M. B., Attisano, L., and Wrana, J. L. (1996) *Cell* **85,** 489–500
20. Nishimura, R., Kato, Y., Chen, D., Harris, S. E., Mundy, G. R., and Yoneda, T. (1998) *J. Biol. Chem.* **273,** 1872–1879
21. Nakao, A., Imamura, T., Souchelnytskyi, S., Kawabata, M., Ishisaki, A., Oeda, E., Tamaki, K., Hanai, J.-I., Heldin, C.-H., Miyazono, K., and ten Dijke, P. (1997) *EMBO J.* **16,** 5353–5362
22. Tsukazaki, T., Chiang, T. A., Davison, A. F., Attisano, L., and Wrana, J. L. (1998) *Cell* **95,** 779–791
23. Arias, J., Alberts, A. S., Brindle, P., Claret, F. X., Smeal, T., Karin, M., Feramisco, J., and Montminy, M. (1994) *Nature* **370,** 226–229
24. Dudley, A. T., Lyons, K. M., and Robertson, E. J. (1995) *Genes Dev.* **9,** 2795–2807
25. Luo, G., Hofmann, C., Bronckers, A. L. J. J., Sohocki, M., Bradley, A., and Karsenty, G. (1995) *Genes Dev.* **9,** 2808–2820
26. McKnight, G. S. (1991) *Curr. Opin. Cell Biol.* **3,** 213–217
27. Eresh, S., Riese, J., Jackson, D. B., Bohmann, D., and Bienz, M. (1997) *EMBO J.* **16,** 2014–2022
28. Topper, J. N., DiChiara, M. R., Brown, J. D., Williams, A. M., Falb, D., Collins, T., and Gimbrone, M. A. J. (1998) *Proc. Natl. Acad. Sci. U. S. A.* **95,** 9506–9511
29. Feng, X.-H., Zhang, Y., Wu, R.-Y., and Derynck, R. (1998) *Genes Dev.* **12,** 2153–2163
30. Janknecht, R., Wells, N. J., and Hunter, T. (1998) *Genes Dev.* **12,** 2114–2119
31. Pouponnot, C., Jayaraman, L., and Massagué, J. (1998) *J. Biol. Chem.* **273,** 22865–22868
32. Zhong, H., SuYang, H., Erdjument-Bromage, H., Tempst, P., and Ghosh, S. (1997) *Cell* **89,** 413–424

EXHIBIT B

1: Pharm Acta Helv. 2000 Mar;74(2-3):265-72. Links

The ciliary neurotrophic factor and its receptor, CNTFR alpha.

Sleeman MW, **Anderson KD**, **Lambert PD**, **Yancopoulos GD**, **Wiegand SJ**.

Regeneron Pharmaceuticals, Tarrytown, NY 10591-6707, USA. mark.sleeman@regpha.com

Ciliary neurotrophic factor (CNTF) is expressed in glial cells within the central and peripheral nervous systems. CNTF stimulates gene expression, cell survival or differentiation in a variety of neuronal cell types such as sensory, sympathetic, ciliary and motor neurons. In addition, effects of CNTF on oligodendrocytes as well as denervated and intact skeletal muscle have been documented. CNTF itself lacks a classical signal peptide sequence of a secreted protein, but is thought to convey its cytoprotective effects after release from adult glial cells by some mechanism induced by injury. Interestingly, mice that are homozygous for an inactivated CNTF gene develop normally and initially thrive. Only later in adulthood do they exhibit a mild loss of motor neurons with resulting muscle weakness, leading to the suggestion that CNTF is not essential for neural development, but instead acts in response to injury or other stresses. The CNTF receptor complex is most closely related to, and shares subunits with the receptor complexes for interleukin-6 and leukemia inhibitory factor. The specificity conferring alpha subunit of the CNTF complex (CNTFR alpha), is extremely well conserved across species, and has a distribution localized predominantly to the nervous system and skeletal muscle. CNTFR alpha lacks a conventional transmembrane domain and is thought to be anchored to the cell membrane by a glycosyl-phosphatidylinositol linkage. Mice lacking CNTFR alpha die perinatally, perhaps indicating the existence of a second developmentally important CNTF-like ligand. Signal transduction by CNTF requires that it bind first to CNTFR alpha, permitting the recruitment of gp130 and LIFR beta, forming a tripartite receptor complex. CNTF-induced heterodimerization of the beta receptor subunits leads to tyrosine phosphorylation (through constitutively associated JAKs), and the activated receptor provides docking sites for SH2-containing signaling molecules, such as STAT proteins. Activated STATs dimerize and translocate to the nucleus to bind specific DNA sequences, resulting in enhanced transcription of responsive genes. The neuroprotective effects of CNTF have been demonstrated in a number of in vitro cell models as well as in vivo in mutant mouse strains which exhibit motor neuron degeneration. Intracerebral administration of CNTF and CNTF analogs has also been shown to protect striatal output neurons in rodent and primate models of Huntington's disease. Treatment of humans and animals with CNTF is also known to

induce weight loss characterized by a preferential loss of body fat. When administered systemically, CNTF activates downstream signaling molecules such as STAT-3 in areas of the hypothalamus which regulate food intake. In addition to its neuronal actions, CNTF and analogs have been shown to act on non-neuronal cells such as glia, hepatocytes, skeletal muscle, embryonic stem cells and bone marrow stromal cells.

PMID: 10812968 [PubMed - indexed for MEDLINE]

Related Links

- The ciliary neurotrophic factor receptor alpha component induces the secretion of and is required for functional responses to cardiotrophin-like cytokine. [EMBO J. 2001]
- Signaling pathways recruited by the cardiotrophin-like cytokine/cytokine-like factor-1 composite cytokine: specific requirement of the membrane-bound form of ciliary neurotrophic factor receptor alpha component. [J Biol Chem. 2001]
- The tripartite CNTF receptor complex: activation and signaling involves components shared with other cytokines. [J Neurobiol. 1994]
- Signaling pathway of ciliary neurotrophic factor in neuroblastoma cell lines. [Med Pediatr Oncol. 2001]
- Agonistic and antagonistic variants of ciliary neurotrophic factor (CNTF) reveal functional differences between membrane-bound and soluble CNTF alpha-receptor. [J Biol Chem. 1997]

See all Related Articles...

Display AbstractPlus Show 20 Sort By Send to

Write to the Help Desk
NCBI | NLM | NIH
Department of Health & Human Services
Privacy Statement | Freedom of Information Act | Disclaimer